The Astronomical Journal, 154:31 (11pp), 2017 July https://doi.org/10.3847/1538-3881/aa6d5e

The Discovery of λ Bootis Stars: The Southern Survey I

R. O. Gray[1], Q. S. Riggs[1], C. Koen[2], S. J. Murphy[3,4], I. M. Newsome[1], C. J. Corbally[5], K.-P. Cheng[6], and J. E. Neff[7]
[1] Department of Physics and Astronomy, Appalachian State University, Boone, NC 26808, USA
[2] Department of Statistics, University of the Western Cape, Private Bag X17, Bellville, 7535 Cape Town, South Africa
[3] Sydney Institute for Astronomy (SIfA), School of Physics, University of Sydney, NSW 2006, Australia
[4] Department of Physics and Astronomy, Stellar Astrophysics Centre, Aarhus University, DK-8000 Aarhus C, Denmark
[5] Vatican Observatory Research Group, Steward Observatory, Tucson, AZ, 85721-0065 USA
[6] California State University, Fullerton, Fullerton, CA, USA
[7] National Science Foundation, Arlington, VA, USA
Received 2017 March 7; revised 2017 April 6; accepted 2017 April 7; published 2017 June 29

Abstract

The λ Boo stars are a class of chemically peculiar Population I A-type stars characterized by under-abundances of the refractory elements, but near-solar abundances of carbon, nitrogen, oxygen, and sulfur. There is some evidence that λ Boo stars have higher frequencies of "bright" debris disks than normal A-type stars. The discovery of four exoplanets orbiting HR 8799, a λ Boo star with a resolved debris disk, suggests that the λ Boo phenomenon may be related to the presence of a dynamic debris disk, perhaps perturbed by migrating planets. However, only 64 λ Boo stars are known, and those stars were discovered with different techniques, making it problematic to use that sample for statistical purposes, including determining the frequency of debris disks. The purpose of this paper is to derive a new sample of λ Boo stars using a technique that does not lead to biases with respect to the presence of infrared excesses. Through spectroscopic observations in the southern hemisphere, we have discovered 33 λ Boo stars and have confirmed 12 others. As a step toward determining the proportion of λ Boo stars with infrared excesses, we have used *WISE* data to examine the infrared properties of this sample out to 22 μm. On this basis, we cannot conclude that λ Boo stars have a greater tendency than normal A-type stars to show infrared excesses. However, observing this sample at longer wavelengths may change that conclusion, as many λ Boo debris disks are cool and do not radiate strongly at 22 μm.

Key words: circumstellar matter – stars: chemically peculiar – stars: early-type – stars: emission-line, Be – stars: evolution

Supporting material: machine-readable tables

1. Introduction

The λ Boo stars are a class of chemically peculiar Population I A-type stars characterized by up to 2 dex under-abundances of the refractory elements, but with near-solar abundances of carbon, nitrogen, oxygen, and sulfur. The class was first discovered by Morgan et al. (1943) and named after the brightest prototype, λ Boo, which is also one of the more extreme members of the class. Unfortunately, over the decades, because the class was loosely and variously defined in the literature, it accreted a variety of unrelated peculiar stars.

Gray (1988) attempted to rectify that situation, and went on to identify a homogeneous set of sixteen λ Bootis stars that have served as the basis for much of the subsequent research on the class. More stars were added to this original set through the efforts of Gray (1991), Gray & Corbally (1993, 1998, 2002), Paunzen & Gray (1997), Gray & Kaye (1999), Paunzen et al. (2001), and Paunzen (2001). Other researchers, too numerous to cite, contributed more candidates to the list. By 2015, the field was ripe for a critical re-evaluation. That was provided by Murphy et al. (2015), who surveyed the entire literature for λ Bootis candidate stars and applied a uniform set of criteria to all 212 candidates, resulting in a list of 64 bona fide λ Bootis stars, 103 non-members of the class, and 45 stars for which the membership status remains unclear and can only be evaluated with additional data.

The prevailing hypothesis to explain the under-abundances of the refractory elements (but near-solar abundances of C, N, O, and S) is the accretion of metal-depleted gas from either the interstellar medium or from a circumstellar disk or shell (Venn & Lambert 1990). The mechanism involves the precipitation of the refractory elements into dust grains, which are blown away by radiation pressure (Venn & Lambert 1990; Waters et al. 1992). The remaining metal-depleted gas is then accreted onto the stellar surface. With a sufficiently high accretion rate ($\gtrsim 10^{-13}\,M_{\odot}\,\mathrm{yr}^{-1}$) coupled with a lack of a deep surface convection zone, that accreted gas can lead to observable under-abundances (Charbonneau 1993). Indeed, a sizeable fraction of λ Boo stars show discrete, sharp, variable absorption components in the cores of the Ca II K-line and the Na I D lines, similar to those observed in the spectrum of the protoplanetary-disk star β Pic (Gray 1988; Holweger & Stürenburg 1991; Holweger & Rentzsch-Holm 1995; Griffin et al. 2012). These components are often interpreted as arising from Falling Evaporating Bodies (cf. Lagrange-Henri et al. 1988), which may be massive comets or ablated atmospheres from hot Jupiters (Jura 2015).

A significant fraction of known λ Boo stars show infrared excesses, which Draper et al. (2016) have convincingly demonstrated are caused by debris disks and not by interstellar-medium bow waves. What proportion of λ Boo stars show infrared excesses is a matter of debate. Paunzen et al. (2003) estimated that proportion to be approximately 23%, similar to that of A-type stars in general (Thureau et al. 2014). Draper et al. (2016) argued that the Paunzen estimate may be too conservative and calculated from the Su et al. (2006) 123-star *Spitzer* sample (of which 13 are λ Boo stars)

that the percentage of λ Boo stars with excesses detected at 24 or 70 μm may be as high as 77%. Confirmation of the association of bright debris disks with the λ Boo class would have profound implications for our understanding of the λ Boo stars and would suggest that the λ Boo class represents a phase in the evolution of A-type stars characterized by dynamic debris disks, perhaps perturbed by the migration of massive planets. In this context, it is worthy of note that the dusty λ Boo star, HR 8799 (Gray & Kaye 1999), is host to the first *imaged* exoplanets (Marois et al. 2008). In addition, Folsom et al. (2012), as well as a number of other authors, have discovered Herbig Ae stars with λ Boo abundance patterns. Kama et al. (2015) suggested that the gravitational effects of giant planet(s) in the protoplanetary disks of λ Boo Herbig Ae stars block the accretion of metal-rich dust, but allow the accretion of gas-phase carbon and oxygen. On the other hand, there are a number of known λ Boo stars that do not show evidence for debris disks. Presumably, those diskless λ Boo stars are simply older, but this is difficult to reconcile with the accretion scenario, as the lifetime of the λ Boo phase should be short-lived ($\sim 10^6$ yr, Turcotte & Charbonneau 1993) once accretion stops. This raises the question of whether there are multiple channels to the λ Boo "state" (Murphy & Paunzen 2017).

The current sample of 64 known λ Boo stars is not adequate to address these questions, first, because it is difficult to know whether that sample is biased with respect to the presence of infrared excesses, and second, because many of those stars are bright and are thus saturated in surveys, such as the *GALEX*, 2MASS, and *WISE* surveys. The main purpose of this paper and further papers in this series is to increase the number of known λ Boo stars in a way that does not include bias with respect to the presence of infrared excesses.

2. Sample Selection

λ Bootis stars constitute about 2% of the field A-type stars (Gray & Corbally 2002), and so a general spectroscopic survey of A-type field stars is unlikely to turn up a substantial number of new λ Boo stars without considerable effort. However, we estimate that many hundreds of λ Bootis stars with $7.5 \leqslant V \leqslant 9.5$ still await discovery. Stars in this magnitude range should have good, unsaturated photometry in the 2MASS, *GALEX*, and *WISE* databases. We are currently conducting an observing program to discover some of these stars in the northern sky with the VATTSpec spectrograph on the Vatican Advanced Technology Telescope on Mt. Graham, Arizona. In the southern hemisphere, we have obtained spectra of λ Bootis candidates with the ANU 2.3 m telescope at Siding Spring Observatory, Australia and with the South African Astronomical Observatory (SAAO) 1.9 m telescope. This paper reports on the stars observed at SAAO.

An important long-term goal of this project is to estimate the percentage of λ Boo stars that show detectable infrared excesses. This means that the strategy that we adopt to pre-select λ Boo candidates for spectroscopic identification should not bias that determination. In previous studies (cf. Gray 1991), λ Boo candidates were selected on the basis of their location in the Strömgren $[m_1]$, $[c_1]$ diagram, but that technique, although presumably unbiased with respect to infrared excesses, has mostly run its course because of the limited number of A-type stars that have been observed on the Strömgren *uvby* system. We are actively researching λ Boo candidates identified by the MKCLASS automatic spectral classification program in the LAMOST-*Kepler* project (Gray et al. 2016); the results from that effort will be reported elsewhere. Unfortunately, many of those stars are too faint to be easily observed down to photospheric flux levels in the far-infrared, even with future space missions.

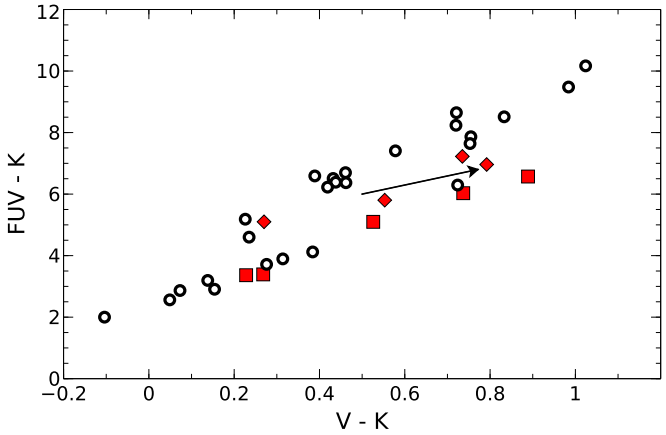

Figure 1. Normal A-type stars (open circles) and λ Bootis stars (red squares and diamonds) are plotted in a color–color diagram. The ordinate is a color formed from the difference of the *GALEX* far-ultraviolet magnitude and the 2MASS K magnitude, and the abscissa is the $V - K$ color. The FUV magnitudes for the λ Bootis stars indicated by the diamonds have been computed by numerical integration of *IUE* spectra, using the *GALEX* FUV passband and transformed to the *GALEX* system. It is clear that the λ Bootis stars, with one exception, lie on or near the lower envelope of the distribution of A-type stars in this diagram, and thus exhibit, for a given $V - K$ color, an FUV excess relative to most normal A-type stars. The arrow shows the reddening vector for $E(B - V) = 0.1$.

λ Bootis stars, because they are metal-weak, have reduced line blanketing in the ultraviolet, and so should all be characterized by near and far-UV excesses relative to normal A-type stars (cf. Gray & Corbally 2009). The *GALEX* spacecraft (Martin et al. 2005) carried out an all-sky survey (except for fields near the Galactic equator) in two ultraviolet bands—the near-ultraviolet (NUV, $\lambda_{\rm eff} = 2271$ Å) and the far-ultraviolet (FUV $\lambda_{\rm eff} = 1512$ Å). A-type stars in the desired magnitude range are almost all saturated in the NUV band but not in the FUV band. Known λ Bootis stars that have an unsaturated *GALEX* FUV magnitude, or that have *IUE* spectra (Nichols & Linsky 1996) that can be numerically integrated to yield an equivalent FUV magnitude have been plotted in Figure 1, along with a number of normal A-type stars against their $V - K$ colors. It is clear that most λ Bootis stars lie on or near the lower envelope of the distribution of A-type stars in this diagram, and thus, for a given $V - K$ color, exhibit "bluer" FUV $- K$ colors (FUV excesses) relative to most normal A-type stars. This suggests the following candidate selection strategy: cross-correlate the TYCHO catalog (which has V and B photometry, Høg et al. 2000) and the 2MASS Point Source catalog (which supplies K-band photometry, Skrutskie et al. 2006) with the *GALEX* photometry catalog to find A-type stars with FUV excesses for their $V - K$ colors. This method is not fool-proof, as can be seen from Figure 1 where some apparently normal A-type stars have FUV-K colors similar to λ Bootis stars. In addition, heavily reddened stars will appear to have FUV excesses because of the slope of the reddening line in the $(\mathrm{FUV} - K)/(V - K)$ diagram. However, because the *GALEX* survey largely avoided the Galactic equator region, this is not a large problem for this sample. Stars with hot companions, such as white dwarfs or OB subdwarfs, or

confused sources, might also be picked up with this method. In general, however, this selection strategy should significantly increase the percentage of λ Bootis stars in the observational sample in a way that will not seriously bias the statistics with respect to infrared excesses. Stars selected with this method are referred to in this paper as the "TYCHO sample."

The other sample of stars reported in this paper includes a few known λ Boo stars, λ Boo candidates from the Murphy et al. (2015) paper in the "uncertain membership" categories (see above), and a number of stars selected with the Strömgren $[m_1]$–$[c_1]$ method. This sample is referred to in this paper as the "miscellaneous sample."

3. Observations

Observations were carried out with the SAAO SpCCD grating spectrograph, attached to the SAAO 1.9 m telescope. Grating 6 was employed, which yields a resolution of about 2 Å/2 pixels and a spectral range from 3600 to 5400 Å. Time was granted for four observing runs of about 5 days each in 2013 December, and 2014 March, June, and September, enabling us to cover the entire southern sky. A total of 291 program stars, plus a number of MK standards, were observed over the four runs. The spectra were reduced using standard methods with IRAF.[8] The average signal-to-noise of the spectra is excellent and in most cases exceeds 150. All of the spectra were rectified for classification and analysis purposes.

4. Spectral Classification

A number of MK standard A- and early F-type stars were observed with the same equipment as the program stars. However, the standards so obtained constituted a grid that was too sparse—especially in the mid A-type stars—for precise classification of the program spectra. We therefore supplemented those standards with standard stars drawn from the libr18 standards library of Gray & Corbally (2014).[9] Those standards were observed with the Dark Sky Observatory (Appalachian State University, North Carolina) GM spectrograph and have a spectral resolution of 1.8 Å/2 pixels and a spectral range from 3800 to 4600 Å. Because those spectra have a slightly higher resolution than the program standards, they were convolved with a Gaussian to match the resolution of the SAAO spectra.

The spectral classification of λ Bootis stars is described in detail in Gray & Corbally (2009). In summary, because λ Bootis stars are metal-weak, a spectral type based on the hydrogen lines (the hydrogen-line spectral type) is "later" than spectral types based on the Ca II K-line and the general metallic-line spectrum. Thus, the full spectral type of a λ Bootis star consists of those three spectral types, a luminosity class, and the designation "λ Boo." For instance, the spectral type for the classical λ Boo star HR 4881 is "F0 V kA1mA1 λ Boo" where "F0" is the hydrogen-line type, "kA1" represents the Ca II K-line type, and "mA1" the metallic-line type. Stars that appear to be mild λ Boo stars are designated as "(λ Boo)." The best indicator of the effective temperature of the star is the hydrogen-line type, that is, HR 4881 is an F0 star, and not an A1 star. Indeed, the metallic-line spectrum, even though it has the same general strength as that of an A1 star, appears decidedly peculiar compared to that standard. For instance, the Ca I 4226 Å resonance line, which grows rapidly in strength with declining effective temperature, is strong relative to that of the A1 spectrum, while the Mg II 4481 Å line is clearly weak. Both of those effects are related to the fact that the star has a lower effective temperature than normal A1 stars.

Some confusion is possible between λ Bootis stars and two other classes—the A-type horizontal branch (HB) stars and metal-weak, thick-disk early F-type stars. In the first case, Gray & Corbally (2009) have discussed how the HB stars may be distinguished from λ Bootis stars using high-S/N classification-resolution spectra, such as those employed for this study. Radial velocities can also help to distinguish between these two classes. The confusion between late-type (F1 and later) λ Bootis stars and metal-weak early F-type stars of the thick disk is more problematic. Theoretically, the frequency of λ Bootis stars should decline precipitously for spectral types later than F0 because of the deepening surface convective zone, which will serve to erase the surface under-abundances. On the other hand, the number of stars in the thick disk rises sharply for spectral types later than F0 (Gray 1989). This means there is a overlap between the two populations (F1–F3) where it is difficult to distinguish between the two classes using the techniques of spectral classification. Detailed abundance studies should be definitive, as the λ Bootis star will have near-solar abundances of carbon, nitrogen, oxygen, and sulphur. Cheng et al. (2017) have recently come up with a C I/Mg II line ratio that shows some promise in distinguishing late-type λ Boo stars from other metal-weak stars. They point out two late-type λ Boo candidates, HD 4158 and HD 106233 (F2 and F3 hydrogen-line types respectively) that are strongly indicated as λ Boo stars by their criterion. Radial velocities may also help to distinguish λ Boo stars from thick-disk stars, although see Paunzen et al. (2014). The presence of an infrared excess should point to a λ Bootis classification, because there is no reason to expect extensive dust around an old, thick-disk dwarf star, unless, for instance, a companion of that star has recently undergone the planetary-nebula phase. But we expect such a contingency to be rare. We will investigate using the presence of IR excesses as a λ Boo criterion in the discussion section. The F1–F3 λ Boo candidates will be termed in this paper "late-type" λ Boo stars, with a "?" appended to their λ Boo classifications to indicate uncertainty about their exact status.

Using the criteria described above, we have classified all of the stars in the Tycho and miscellaneous samples. The spectral types for the TYCHO sample are listed in Table 1, and those for the miscellaneous sample in Table 2. Table 2 also records in the "Notes" column an indication of why the star was observed for this project. Stars with 1, 2, 3, or 4 in the Notes column have all been classified in the literature as λ Bootis stars, but have been judged as "member, probable member, uncertain member, or non-member" respectively of the λ Boo class by Murphy et al. (2015). Stars with "u" in the Notes column have been selected as λ Boo candidates with the Strömgren $[m_1]$–$[c_1]$ method.

This project has led to the discovery of 33 λ Boo stars, including a number of late-type λ Boo candidates. Of these stars, 24 are from the Tycho sample, and 9 were selected as candidates using the Strömgren $[m_1]$–$[c_1]$ technique. These new discoveries are among the main results of this paper. In addition, 12 stars in Murphy et al.'s probable, uncertain, or

[8] IRAF is distributed by the National Optical Astronomy Observatory, which is operated by the Association of Universities for Research in Astronomy, Inc. under cooperative agreement with the National Science Foundation.

[9] http://www.appstate.edu/~grayro/mkclass/

Table 1
TYCHO Sample: Spectral Types, Models, $E(B-V)$, and IR Excesses

TYC	Other ID	SpT	Model Used			$E(B-V)$	IR?	Notes
			$T_{\rm eff}$	log g	[M/H]			
4712 00625 1	HD 21417	A8 III	7450	3.6	0.0	0.020	n	···
4725 01108 1	HD 27750	kA7hF0mF0 IV	7300	4.2	0.0	0.103	n	···
4737 00609 1	HD 31681	A5 IV(n)	7900	4.2	0.0	0.050	n	···
4747 00429 1	HD 29492	A9 V	7600	4.2	0.0	0.058	n	···
4835 00773 1	BD-01 1818	F1 V	7050	4.2	0.0	0.000	n	···

(This table is available in its entirety in machine-readable form.)

non-member categories have been confirmed as λ Boo stars or "late-type" λ Boo candidates. This makes a total of 45 "new" λ Boo stars (although the late-type candidates will need to be confirmed with other techniques), a 70% increase in the number of confirmed λ Boo stars over those identified in Murphy et al. (2015).

5. Basic Physical Parameters, Reddening, and Infrared Excesses

The presence of infrared excesses in the program stars (see the next section) can be determined by comparing far-infrared data from archival sources (such as the *WISE*, *IRAS*, and *Spitzer space telescopes*) with theoretical spectral energy distributions based on stellar atmosphere models. This requires knowledge of the basic physical parameters and reddening of the program stars. We have estimated these parameters with the following procedure:

5.1. Basic Physical Parameters and Reddening

A library of synthetic rectified spectra with effective temperatures spanning 6500–11,500 K (spacing 50 K) was calculated for $\log g = 3.3$, 3.6, 4.0, and 4.2, with metallicities of [M/H] = +0.5, +0.2, 0.0, −0.2, −0.5, −1.0, −1.5, and −2.0. These spectra have been convolved with a Gaussian linespread function to duplicate the resolution of the SAAO spectra. The synthetic spectra were computed with the spectral synthesis program SPECTRUM (Gray & Corbally 1994) using stellar atmosphere models computed with the ATLAS9 program (Castelli & Kurucz 2003). The spectral line list employed was `lukeall2.iso.lst`, which may be obtained on the SPECTRUM website.[10]

The normal methods used to determine the physical parameters from high-resolution spectra cannot be employed with the relatively low-resolution SAAO spectra. One of us (Q.S.R.) has written a computer program (`extractIR`) that, in addition to downloading B and V photometry from Simbad and infrared photometry from IPAC, finds the model, for a given metallicity, with the minimum χ^2 difference with the observed spectrum. Infrared excesses (see below) are then detected by comparing model fluxes with observed fluxes.

The χ^2 fit uses extra weighting for the hydrogen lines (Hβ and Hγ) to ensure a good fit with the hydrogen-line profiles. The χ^2 fit includes only $T_{\rm eff}$ and $\log g$; we have found that including the metallicity ([M/H]) in the fit can lead to spurious solutions because of so-called spectroscopic "degeneracies" in the A-type stars (see discussion in Gray & Corbally 2009). We have found the best way to proceed is to begin with solar metallicity models, examine the fit between the observed and synthetic spectrum visually, and then adjust the metallicity and re-run the fit until the best match is found. The visual inspection of the match between the theoretical spectrum and the observed spectrum, using the methods of spectral classification, helps to break the spectroscopic degeneracy.

The photometric fluxes considered in this paper (Johnson B, V, 2MASS J, H, and K, and *WISE* W1, W2, W3, and W4) are dereddened with a combination of the Fitzpatrick reddening law (Fitzpatrick 1999) and the mid-infrared extinction law of Xue et al. (2016). The $E(B-V)$ excess is estimated by considering the intrinsic color that corresponds to a given spectral type. We have used the spectral-type "running number" (see http://www.appstate.edu/~grayro/mkclass/ for a tabulation of the running number) and the Johnson $B-V$ indices of normal A-type stars (B8–F2) within 40pc of the Sun (Gray et al. 2003, 2006) to derive a calibration that predicts the intrinsic $B-V$ index of the star to an accuracy of ±0.03 mag:

$$(B-V)_0 = -0.176 - 0.0130{\rm RN} + 0.001455{\rm RN}^2 \quad (1)$$

where RN is the spectral-type running number. Empirical metallicity corrections to that calibration have been derived by considering both metal-rich (Am-type) and metal-poor (λ Bootis) stars from those same references. We find the following corrections: for [M/H] $\leqslant -1.0$, subtract 0.04 from $(B-V)_0$, for [M/H] = −0.5, subtract 0.02, for [M/H] = −0.2, subtract 0.01, for [M/H] = +0.2, add 0.01, and for [M/H] = +0.5, add 0.03. These corrections are of minor importance for our application, as the infrared Rayleigh–Jeans tail of A-type stars is insensitive to both $T_{\rm eff}$ and metallicity as well as gravity (see Figure 2).

A complication to the reddening determination is that many of our program stars have only Tycho-2 (Høg et al. 2000) B and V magnitudes (hereafter $B_{\rm T}$ and $V_{\rm T}$). The Tycho-2 photometric system deviates significantly from the Johnson system. The transformation of $B_{\rm T}$ and $V_{\rm T}$ magnitudes to Johnson B and V is controversial and involves color terms, so to avoid this difficulty, we have used the same set of normal A-type stars to derive a calibration similar to Equation 1 but using the Tycho-2 $(B_{\rm T}-V_{\rm T})$ color. This calibration may be used to derive $E(B_{\rm T}-V_{\rm T})$:

$$(B_{\rm T}-V_{\rm T})_0 = 0.223 - 0.0476{\rm RN} + 0.002248{\rm RN}^2. \quad (2)$$

The correspondence between $E(B_{\rm T}-V_{\rm T})$ and $E(B-V)$ is very close; to verify this, we have used the passbands tabulated in Bessell & Murphy (2012) to calculate values of $(B-V)$ and $(B_{\rm T}-V_{\rm T})$ for a number of synthetic flux models representing dwarf A-type stars ($T_{\rm eff}$ = 7000–10,000 K). We employed the Fitzpatrick reddening law to redden those flux models by

[10] http://www.appstate.edu/~grayro/spectrum/spectrum.html

Table 2
Miscellaneous Sample: Spectral Types, Models, $E(B-V)$, and IR Excesses

HD	Other ID	SpT	Model Used			$E(B-V)$	IR?	Notes
			$T_{\rm eff}$	$\log g$	[M/H]			
HD 2884	β^1 Tuc	B9.5 Va	10800	4.2	−0.2	0.009	n	u
HD 2885	β^2 Tuc	A3 IV	8300	3.3	0.0	0.033	⋯	u
HD 3736	⋯	A6 IV	7700	4.0	0.0	0.000	n	u
HD 3922	⋯	F0 V(n) kA6mA5 λ Boo	7400	4.2	−0.5	0.000	n	u
HD 11413	BD Phe	F0 V kA2mA2 λ Boo	7400	4.2	−1.0	0.000	n	1, u

(This table is available in its entirety in machine-readable form.)

$A_V = 0.3225$ $(E(B-V) = 1.0)$ and then computed the resulting values of $E(B_{\rm T}-V_{\rm T})/E(B-V)$. That ratio is unity to within 1% in the realm of the A-type stars.

Bessell & Murphy (2012) also published zero-points for the Tycho $B_{\rm T}$ and $V_{\rm T}$ photometry, enabling the direct calculation of stellar fluxes in those bands.

A remaining problem with employing Tycho-2 photometry to determine reddenings is that there is a small proportion of stars for which the tabulated photometry is clearly spurious, especially in the $B_{\rm T}$ band. This can lead to unreasonably large values for $E(B-V)$. When the calculated reddening is too large, the dereddened *WISE* fluxes lie systematically *below* the model fluxes (we normalize the model fluxes to the dereddened stellar flux in the 2MASS *J* band). In some cases, the calculated reddening may even exceed the Galactic line-of-sight reddening based on *IRAS* 100 μm emission (Schlafly & Finkbeiner 2011). When it is clear the reddening is too large, we manually adjust the reddening so that the W1 and W2 fluxes agree with the theoretical fluxes. In all cases, this reduces the reddening to well below the Galactic line-of-sight reddening.

5.2. Infrared Excesses

Infrared excesses out to 22 μm are detected by comparing the stellar fluxes in the *WISE* W1, W2, W3, and W4 bands with theoretical fluxes based on the models selected with the procedure described in the above paragraphs. These theoretical fluxes are calculated with SPECTRUM using the `lukeall2.iso.lst` line list extended to 100 μm with the atomic-line list found on Kurucz CD23 (Kurucz & Bell 1995). Flux comparisons are made by normalizing the theoretical flux spectrum to the stellar flux in the 2MASS *J*-band, except in those few instances where there is clear emission in that band, in which case the normalization is made with the *V*-band. Normalizing to the *J*-band is preferable to the *V*-band for many of our stars because of the discussed problems with the Tycho photometry. Infrared excesses are recorded in the form of a flux ratio, $(F_{\rm observed}-F_{\rm theoretical})/F_{\rm theoretical}$, and the significance of those excesses is judged on the basis of the errors recorded for the *WISE* photometry.

We have detected infrared excesses arising from two types of sources. A number of our stars show excesses consistent with the presence of a cooler stellar companion. Most of these stars are known spectroscopic, speckle, or eclipsing binaries, and naive fitting of the excesses with a blackbody yields a source temperature and luminosity consistent with a star. The second type of infrared-excess source shows excesses consistent with a debris disk. For many of the stars in the miscellaneous sample, these excesses have already been investigated in the literature (see comments in Section 6.2.1). The others (including from the Tycho sample) generally show excesses only in *WISE* bands W3 and W4, or sometimes only in W4 (or, in other cases, only in W3, if the W4 error is too large), and those excesses are consistent with the presence of a cool debris disk ($T \lesssim 100$ K), although we do not have enough flux points to determine a temperature.

If an excess is detected with a flux ratio >0.1 and $\sigma > 2$, it is indicated with a "*" or a "†" in the "IR?" columns of Tables 1 and 2. The "*" indicates an excess attributable to a debris disk, and the "†" indicates the excess arises from a cooler stellar companion. We have chosen, for the purposes of this paper, the criterion $\sigma > 2$ instead of the usual $\sigma > 3$ in order not to overlook, for the purpose of planning future observations, possibly interesting stars. As it turns out (cf. Draper et al. 2016), many known λ Boo stars have quite cool debris disks that do not radiate strongly at 22 μm, but which do have highly significant excesses at longer wavelengths. The flux ratios and standard deviations for those excesses are recorded, band-by-band, in Tables 3 and 4 for the Tycho sample and the miscellaneous sample, respectively. If no significant excess is detected in the *WISE* bands, that is indicated with a "n" in the "IR?" columns of Tables 1 and 2. All of the program stars were detected in *WISE* bands W1, W2, and W3. Most were detected in W4 (22 μm), but in a minority of cases, the recorded W4 flux is only an upper limit. This has been indicated in the "IR?" column of Tables 1 and 2 with "W4 ↓."

6. Results

6.1. The Tycho Sample

There are 207 stars in the Tycho sample, and among those we have identified 25 λ Boo stars (including 3 late-type λ Boo stars and one previously known λ Boo star), 32 Am stars, 5 Ap stars, 1 shell star, and 3 composite spectra. The remaining stars (139) can be considered "normal" A-type stars. Thus, our selection method yielded 12% λ Boo stars, a much higher percentage than expected from a general field star survey (2%). The percentage of Am stars (16%) is about half expected from a field star survey (34% Abt 1981), probably because our selection criteria were biased toward metal-weak stars.

Of the 25 λ Boo stars identified, 5 have only upper limits on the W4 flux. Among the remaining 20 λ Boo stars, 4 show significant infrared excesses (attributable to debris disks) in one or more *WISE* bands, for a proportion of 20 ± 10%. None of the "late-type" λ Boo candidates in this sample show significant infrared excesses. Those stars, however, tend to be among the fainter stars in the sample, and this means larger uncertainties on the *WISE* fluxes. Indeed, of the 5 λ Boo stars with only upper limits on the W4 flux, 4 have hydrogen-line spectral types of F0 and later.

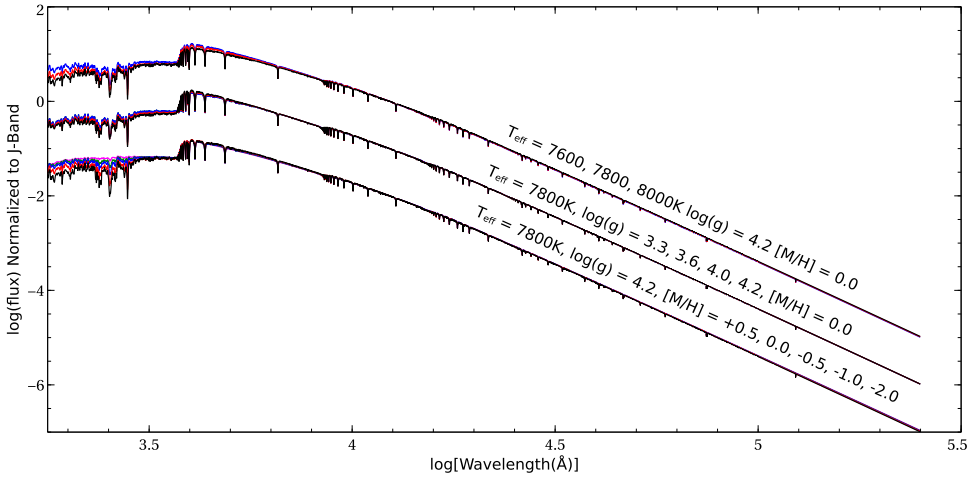

Figure 2. Model flux distributions for various ranges of $T_{\rm eff}$, $\log g$, and metallicity, demonstrating the insensitivity of the infrared Rayleigh–Jeans tail to changes in those physical parameters. All of these flux distributions are normalized to unity at the effective wavelength of the 2MASS *J*-band, 1.235 μm, but have been displaced by one unit in the log for clarity. The top plot shows the variation in the flux distributions for effective temperatures in the mid-A star range. Differences in the UV are evident, but the infrared Rayleigh–Jeans tails practically coincide. Much the same can be seen for the middle plots, which explore changes with $\log g$. Likewise for the lower plots for metallicity. However, for the metallicity plots, note the large differences in line blanketing in the ultraviolet. Flux distributions were computed with SPECTRUM using Castelli & Kurucz (2003) models.

Of the 139 normal A-type stars observed, 18 have only upper limits on the W4 flux. Of the remaining 121 stars, 18 show significant infrared excesses (attributable to debris disks) in one or more *WISE* bands for a total of 14.9 ± 3.5%. With the quoted errors, we cannot, therefore, on the basis of the Tycho sample, conclude that λ Boo stars have a higher frequency of occurrence of infrared excesses out to 22 μm (*WISE* band W4) than the normal A-type stars. This, however, does not necessarily contradict the conclusion of Draper et al. (2016), that a much higher proportion of λ Boo stars show infrared excesses, because most λ Boo debris disks are quite cool and do not radiate strongly shortward of 22 μm (cf. Draper et al. 2016, Figure 3). Unfortunately, none of the Tycho sample stars have *Spitzer* or other far-infrared photometry.

Figure 3 shows an HR diagram for the Tycho λ Boo stars. Consistent with earlier findings (cf. Paunzen et al. 2002, 2014; Murphy & Paunzen 2017), the λ Bootis stars in the Tycho sample appear to lie between the zero-age main sequence (ZAMS) and the terminal-age main sequence (TAMS). Another interpretation is that these stars are still in the pre-main-sequence phase, but (with one possible exception) lack of association with star formation regions or other young stars suggests that, on the contrary, all of these stars are in the hydrogen-burning phase of evolution. A minority of the stars in the sample (6) appear to be ZAMS or near-ZAMS objects. Interestingly, the presence of infrared excesses out to 22 μm (indicated by red "halos" around the points in Figure 3) does not appear to be confined to ZAMS objects.

6.1.1. Notes on Individual Stars in the Tycho Sample

TYC 5478-00796-1: A δ Sct variable λ Boo star (Nichols et al. 2010).

TYC 5825-01038-1: = HD 220687, an eclipsing binary with a δ Sct component (Pigulski & Michalska 2007). The infrared excess is almost certainly due to the cooler component.

TYC 5849-01699-1: = HD 4158, a previously known late-type λ Boo star. See discussion in Section 4.

TYC 6040-01051-1: An F0-type shell star. Fe II 4923, 5018, and 5169 Å (multiplet 42) are enhanced.

TYC 6948-0035901: = HD 205961, an Ap star with a large infrared excess at the *WISE* W4 band and smaller excesses in the other bands.

TYC 6469-01030-1: A composite-spectrum star. Matijevič et al. (2010) (the RAVE survey) list this as a double-lined spectroscopic binary.

TYC 6701-00658-1: A metal-weak A-type star (probably not a λ Boo star, but more investigation is needed) that was detected as a far-UV source with the FAUST telescope (Bowyer et al. 1995).

TYC 7286-01381-1: A mild λ Boo star found in the region of the Sco-Cen association.

TYC 7776-01164-1: An A9 λ Boo star showing significant IR excesses in the W3 and W4 *WISE* bands.

TYC 8198-01674-1: Either a composite spectrum (Simbad gives no indication of duplicity) or a metal-weak F0 V star showing Am characteristics (the K-line type is earlier than the metallic-line type). The similarity of the spectral type to TYC 6469-01030-1 suggests a composite spectrum is more likely.

TYC 8754-01226-1: An A3 λ Boo star showing a significant IR excess in the W4 band.

TYC 8918-01556-1: Another possible composite-spectrum star with a spectral type of F0 V kA2mA5. If normalized to the 2MASS *J* band, it appears to show small but significant IR excesses in all of the *WISE* bands; if normalized to the Tycho V_T band, those small IR excesses extend to the 2MASS *J*, *H*, and *K* bands. These excesses most likely arise from a somewhat cooler companion and not a debris disk. The *Gaia* parallax (4.419 ± 0.264 mas, *Gaia* Collaboration et al. 2016a, 2016b) yields $M_V = 2.55 \pm 0.12$, entirely consistent with the F0 V spectral type. The weak Ca II line relative to the general metallic-line spectrum suggests a composite spectrum. Another possibility is a metal-weak F0 dwarf with Am characteristics (see *TYC 8198-01674-1* above).

TYC 9192-00761-1: An apparently normal A5 V star that shows significant IR excesses in the W3 and W4 bands.

Table 3
TYCHO Sample IR Excesses[a]

TYC	SpT	JHK[b]	W1	W2	W3	W4	Notes[c]
4868 00435 1	F1 IV	⋯	⋯	⋯	⋯	0.78, 2.1	⋯
4925 01350 1	A8 V	J? HK	0.16, 6.8	0.18, 8.4	0.25, 9.9	⋯	†?
4999 01159 1	A3 IV-V	⋯	⋯	⋯	⋯	0.93, 2.9	SB
5010 00685 1	F0 IV-V	⋯	⋯	⋯	0.12, 4.7	1.20, 4.2	⋯
5095 00523 1	A5 V	⋯	⋯	⋯	⋯	0.85, 4.3	⋯
5202 00670 1	A4 V	⋯	⋯	⋯	⋯	1.05, 2.7	⋯
5345 01135 1	A8 IV-V	⋯	⋯	⋯	0.12, 4.2	⋯	⋯
5502 01628 1	A3 IV-V	⋯	⋯	⋯	0.10, 2.7	W4 ↓	⋯
5709 01360 1	A2 Va-	⋯	⋯	⋯	0.13, 4.5	1.38, 3.2	⋯
5713 00778 1	A3 Va	⋯	⋯	⋯	⋯	0.90, 3.4	⋯
5787 00843 1	A7 IV	⋯	⋯	⋯	⋯	0.50, 2.0	⋯
5825 01038 1	A7 V	⋯	0.08, 3.9	0.15, 5.7	0.14, 4.8	⋯	EB,†
5940 00245 1	A2 IV-V	⋯	⋯	⋯	0.20 4.6	W4 ↓	⋯
5952 01751 1	kA4hA6mA6 V	⋯	⋯	⋯	⋯	0.76, 2.2	⋯
6174 01069 1	A7 Vn	⋯	⋯	⋯	⋯	0.20, 2.6	⋯
6241 00232 1	A3 V	⋯	⋯	⋯	⋯	0.69, 2.1	⋯
6516 00647 1	A8 V kA2mA2 λ Boo	⋯	⋯	⋯	1.16, 4.6	0.94, 2.7	⋯
6516 01247 1	A9 V kA2mA2 λ Boo	⋯	⋯	⋯	⋯	0.84, 2.3	⋯
6569 03603 1	A7 V	⋯	⋯	⋯	⋯	0.34, 2.4	⋯
6948 00359 1	A9 Vpn kA3 SrEu	⋯	0.12, 5.1	0.12, 5.9	0.15, 4.8	2.4, 6.1	⋯
7152 00928 1	A7 Vn	⋯	⋯	⋯	⋯	0.91, 3.6	⋯
7776 01164 1	A8 V kA1mA2 λ Boo	⋯	⋯	⋯	0.11, 4.7	0.78, 2.7	*
8275 01316 1	kA1.5hA3mA5 IV	⋯	⋯	⋯	⋯	0.58, 2.1	⋯
8276 01241 1	A4 IV-V	⋯	⋯	⋯	⋯	0.78, 3.1	⋯
8369 00234 1	A3 IV	⋯	⋯	⋯	⋯	1.06, 2.0	⋯
8754 01226 1	A3 IV-V kA1mA0 λ Boo		⋯	⋯	⋯	0.47, 2.4	⋯
8918 01556 1	F0 V kA2mA5 composite?	⋯	⋯	0.11, 5.4	0.10, 4.7	0.54, 2.3	*,†
9192 00761 1	A5 V	⋯	⋯	⋯	0.29, 12.	1.82, 5.9	*
9431 01027 1	A5 V	⋯	⋯	⋯	0.14, 4.5	W4 ↓	⋯

Notes.
[a] The infrared excess in the *WISE* bands, measured as $E = (F_{\rm observed} - F_{\rm theoretical})/F_{\rm theoretical}$), is recorded each column as E, σ, where σ is the number of standard deviations by which the observed flux exceeds the theoretical flux (see the text). W4 ↓ indicates the W4 flux is an upper limit.
[b] If an excess is detected in one or more 2MASS bands, that band is noted in this column. If an excess is detected in the *J*-band, the theoretical flux distribution is normalized to the flux in the Johnson or Tycho *V*-band.
[c] A "*" in this column points to comments on the star in Section 6.1.1. Other annotations refer to the duplicity of the star. A † indicates that the observed infrared excesses can be attributed to the presence of a cooler companion. †? indicates that the infrared excesses are consistent with the presence of a cool companion, although no independent evidence for that companion exists.

6.2. The Miscellaneous Sample

The miscellaneous sample consists of stars from Murphy et al. (2015) with mostly uncertain λ Boo identifications in the literature (including a number of Herbig Ae/Be stars suggested by Folsom et al. 2012, from abundance studies as likely λ Boo candidates) as well as a number of λ Boo candidates identified using the Strömgren $[m_1]$–$[c_1]$ method. There are 84 stars in the miscellaneous sample of which 37 have been classified as λ Boo stars (including 15 late-type λ Boo stars and 6 stars which are Herbig Ae/Be stars). In this sample, 5 stars have only upper limits in the W4 band, none of which are λ Boo stars. Of the 37 λ Boo stars, 18 show a significant IR excess in one or more *WISE* bands, attributable to a debris disk, for a total of 49 ± 11%. If we remove the Ae/Be stars from the sample, of the 31 remaining λ Boo stars, 12 show IR excesses, or 39 ± 11%. The percentage of λ Boo stars showing IR excesses out to 22 μm is thus strikingly larger than in the Tycho sample. However, almost all of those λ Boo stars with IR excesses are drawn from the Murphy et al. (2015) survey of the literature, and so it is likely that that sample is in some way biased toward stars with infrared excesses, but this will need to be investigated with a thorough review of the literature cited in that paper.

It is of interest that the miscellaneous sample contains 2 late-type λ Boo stars that appear to show significant infrared excesses consistent with a debris disk (HD 13755, and HD 142994). The detected infrared excesses are inconsistent with those stars being metal-weak members of the thick disk, and strongly suggest that the λ Boo phenomenon can operate out to a spectral type of F2 and possibly later on the main sequence. Indeed, the latest λ Boo star identified in this sample has a hydrogen-line type of F4 (HD 81290).

Figure 4 shows an HR diagram for the λ Bootis stars in the miscellaneous sample (minus the Herbig Ae stars). The filled circles represent stars selected with the Strömgren $[m_1]$–$[c_1]$ method, and the open squares candidates from Murphy et al. (2015). Again, the λ Boo stars seem to be confined to the region between the ZAMS and the TAMS, and only three of the stars illustrated are true ZAMS objects. In addition, a number of clearly evolved λ Boo stars show evidence for infrared excesses.

Table 4
Miscellaneous Sample IR Excesses[a]

ID	SpT	JHK[b]	W1	W2	W3	W4	Notes[c]
HD 13755	F1 V kA8mA8 (λ Boo)	⋯	⋯	⋯	⋯	0.19, 2.4	*
HD 21688	A9 Vn kA5mA5	⋯	⋯	⋯	⋯	0.12, 3.8	⋯
HD 23828	A7 V kA2.5mA3	JHK	1.17, 27.	1.24, 32.	1.39, 32	1.79, 4.2	Algol †
HD 28548	A3 V kA0.5mA0.5 λ Boo	⋯	⋯	⋯	0.66, 19.	7.73, 15.	⋯
HD 30422	A7 V kA3mA3	⋯	⋯	0.12, 2.4	⋯	0.33, 6.8	⋯
HD 42503	A8 Vn kA2mA2 λ Boo	⋯	⋯	⋯	⋯	0.24 3.9	⋯
HD 68695	A3 Vbe kA0mA0 λ Boo	JHK	12., 15.	21., 40.	122., 72.	1491., 61.	*
HD 81290	F4 V kA3mA3	⋯	⋯	⋯	⋯	0.32 2.3	*
HD 97528	F0 IV: kA2mA3: shell	JHK	0.74, 4.1	1.06, 15.	0.98, 34.	1.55, 15	Algol †
HD 99644	A8 V kA3mA3	⋯	⋯	⋯	0.22, 12.	4.47, 26.	⋯
HD 100546	A0 Vae kB8 λ Boo	see Pascual et al. (2016)					*
HD 101412	A3 Vae kA0mA0 λ Boo	JHK	9.2, 16.	28.5, 18.	208., 109.	887., 91.	*
HD 111786	F0 V kA1mA1 λ Boo	⋯	⋯	0.21, 3.7	⋯	0.49, 11.	⋯
HD 139614	A9 Ve kA5mA5 (λ Boo)	JHK	3.9, 8.8	8.4, 20.	175., 155.	2199., 136.	*
HD 141569	A2 Ve kB9mB9 (λ Boo)		1.0, 7.9	1.0, 22.	6.3, 63.	102., 49.	*
HD 141851	A2 IV-Vn	⋯	⋯	0.68, 3.5	0.37, 18.	0.46, 10.	Dbl †
HD 142666	F0 V shell	JHK	6.0, 5.1	14.6, 7.5	200., 64.	946., 50.	⋯
HD 142994	F2 V kA3mA3 λ Boo?	⋯	⋯	0.14, 4.9	⋯	0.60, 8.7	*
HD 148638	A2 IVn	⋯	⋯	⋯	⋯	0.35, 3.4	⋯
HD 154153	F1 V kA3mA3 λ Boo?	K	1.2, 5.2	0.88, 11.	0.12, 7.6	0.23, 5.5	*
HD 160928	A3 IVn	⋯	⋯	0.22, 2.6	0.18, 4.4	⋯	VB
HD 168740	A8 V kA2mA2 λ Boo	⋯	⋯	0.24, 3.8	⋯	0.14, 3.6	⋯
HD 168947	F0 V kA3mA3 λ Boo	⋯	⋯	⋯	⋯	0.34, 2.3	⋯
HD 169142	F1 Ve kA3mA3 λ Boo	JHK	1.9, 8.7	4.0, 19.	75., 108.	1660., 181.	*
HD 177756	B8.5 V	⋯	⋯	1.2, 3.4	0.22, 22.	⋯	⋯
HD 183007	A7 V kA2mA5 composite?	⋯	⋯	0.19, 2.3	⋯	0.10, 3.2	†?
HD 188164	A6 V kA2mA3	⋯	⋯	0.14, 3.2	⋯	⋯	⋯
HD 193256	A8 Vn kA3mA3 (λ Boo)	⋯	⋯	⋯	⋯	0.32, 3.1	⋯
HD 193281	A2 IV-V	J?HK	1.4, 4.0	1.7, 14.	1.3, 39.	1.5, 18.	VB, †
HD 198160	A3 IV(n)	⋯	⋯	⋯	⋯	0.24, 7.4	⋯
HD210111	A9 V kA2mA2 λ Boo	⋯	⋯	0.16, 2.8	⋯	0.21, 5.1	⋯
HD 213669	F0 V kA2.5mA2.5 λ Boo	⋯	⋯	⋯	⋯	0.22, 3.0	⋯
HD 217883	A2 V (shell)	JHK	0.92, 24.	0.94, 27.	1.2, 29.	1.6, 3.0	†
HD 223352	A0 Van kB9 ((λ Boo))	J? HK	⋯	1.0, 3.7	0.36, 19.	1.1, 22.	EB,†
HD 293815	B9.5 Vne	⋯	0.10, 4.7	0.21, 9.8	15.6, 64.	223., 37.	⋯
HD 294166	A2 Vb	⋯	⋯	0.13, 5.9	0.92, 17.	7.4, 7.2	⋯
BD-03 0357	F0 V kA6mA6	⋯	0.27, 11.	0.28, 12.	0.32, 5.8	W4 ↓	EB?, †?

Notes.
[a] The infrared excess in the *WISE* bands, measured as $E = (F_{\rm observed} - F_{\rm theoretical})/F_{\rm theoretical})$, is recorded each column as E, σ, where σ is the number of standard deviations by which the observed flux exceeds the theoretical flux (see the text).
[b] If an excess is detected in one or more 2MASS bands, that band is noted in this column. If an excess is detected in the *J*-band, the theoretical flux distribution is normalized to the flux in the Johnson or Tycho *V*-band.
[c] A "*" in this column indicates notes on the star in Section 6.2.1. Other annotations refer to the duplicity of the star. A † indicates that the observed infrared excesses can be attributed to the presence of a cooler companion. †? indicates that the infrared excesses are consistent with the presence of a cool companion, although no independent evidence for that companion exists.

6.2.1. Notes on Individual Stars in the Miscellaneous Sample

HD 13755: A late-type λ Boo star showing a small excess in the W4 band. Photometry in that band is given an "A" quality by the AllWISE Source Catalog.

HD 68695: An emission-line Ae star with large IR excesses even in the 2MASS *J*, *H*, and *K* bands (see Table 4). Folsom et al. (2012) carried out an abundance analysis for this star, and found "clear λ Boo peculiarities" with C, N, O, and S abundances that are 1σ above solar and iron peak abundances 2–3σ below solar. Our visual classification of this star concurs with their conclusion that this is an Ae λ Boo star with strong emission at Hβ. Murphy et al. (2015) however, obtained two classification spectra of this star, and found it to be a spectrum variable and concluded that it did not appear to be a λ Boo star. Their spectral type (A3 Ve kA1mA0) is almost identical to ours, however.

HD 81290: F4 V kA3mA3 λ Boo? If this star proves to be a λ Boo star, it will be the latest spectral-type λ Boo star known. K.-P. Cheng (2017, private communication) has noted that HD 81290 has a C I/Mg II ratio (cf. Cheng et al. 2017) that is consistent with a λ Boo designation. Table 4 records an excess in the *WISE* W4 band. However, according to the AllWISE Source Catalog, that excess may be due to a latent image left from a bright source.

HD 100546: Acke & Waelkens (2004) found, from an abundance analysis that this Herbig Ae star has solar nitrogen and oxygen abundances, but ∼1 dex under-abundances of magnesium, silicon, and iron. Our spectrum shows strong emission in the core of Hβ, and asymmetric

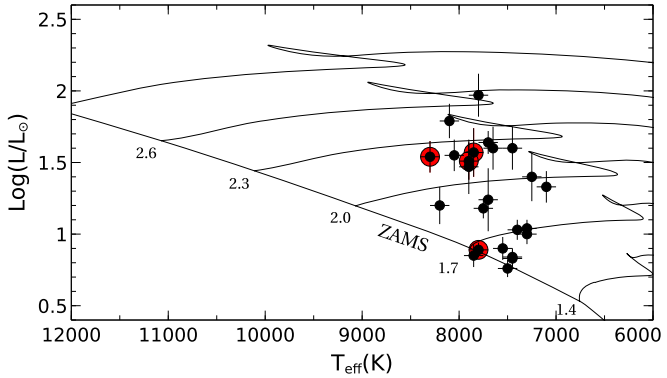

Figure 3. HR diagram of the Tycho λ Boo stars with *Gaia* parallaxes (*Gaia* Collaboration et al. 2016a, 2016b). The temperatures are from Table 1, and the evolutionary tracks ($Z = 0.02$) are from Bressan et al. (2012). Note that all of the λ Boo stars in this sample lie between the ZAMS and the TAMS. Stars showing infrared excesses attributable to a debris disk (see Table 3 and Section 5.2) are indicated with a red "halo" around the data point.

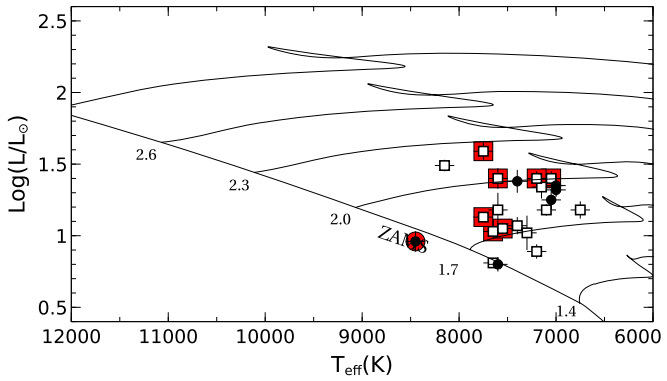

Figure 4. HR diagram of the miscellaneous sample λ Boo stars with *Gaia* parallaxes (*Gaia* Collaboration et al. 2016a, 2016b), excluding the Herbig Ae stars. The temperatures are from Table 2, and the evolutionary tracks ($Z = 0.02$) are from Bressan et al. (2012). The filled circles represent stars discovered with the Strömgren $[m_1]$–$[c_1]$ method, and the open squares represent candidates from Murphy et al. (2015). Note that, as in Figure 3, all of the λ Boo stars in the miscellaneous sample lie between the ZAMS and the TAMS. Stars showing infrared excesses attributable to a debris disk (see Table 4 and Section 5.2) are indicated with a red "halo" around the data point.

infilling of all the higher Balmer lines. The Balmer line wings are consistent with an A0 Va spectral type (although B9.5 Vb is also possible), a helium line spectral type of B9.5, but a B8 metallic-line type (judged from the Ca II K-line and the Mg II 4481 Å line). Thus, we concur with the metal-weak nature of this star, and agree with the λ Boo designation. See Pascual et al. (2016) for a plot of its stellar energy distribution (SED).

HD 101412: Folsom et al. (2012) concluded from an abundance analysis that this Ae star has solar abundances of C, O, and He, with under-abundances in the iron peak elements, characteristic of a λ Boo star. Their analysis agreed closely with that of Cowley et al. (2010), who also noted that its abundance pattern was similar to that of a λ Boo star. Interestingly, this star is magnetic with a longitudinal field of 500 ± 100 G (Folsom et al. 2012). Our spectral type supports its status as a λ Boo star, in agreement with Murphy et al. (2015). Our IR analysis finds strong excesses even in the 2MASS *J*, *H*, and *K* bands.

HD 139614: An abundance analysis by Folsom et al. (2012) found "a clear λ Boo pattern of abundances with solar C, N, and O, and under-abundant iron peak elements in this Ae star. Acke & Waelkens (2004), however, while agreeing with an overall metal-weak nature, did not find evidence for solar abundances for C, N, and O. Folsom et al. (2012) attributed that disagreement to the higher $T_{\rm eff}$ assigned by Acke & Waelkens (8000 K to their 7600 K). Our $T_{\rm eff}$ is in better agreement with Folsom et al. (2012) (7500K), and our spectral type does indeed suggest this is a mild λ Boo star. Murphy et al. (2015) likewise conclude that it is a λ Boo star. Our IR analysis shows strong IR excesses even at 2MASS *J*, *H*, and *K*.

HD 141569: Folsom et al. (2012) find a λ Boo abundance pattern in this Ae star consistent with a mild λ Boo character. Gray & Corbally (1998) classified this star as metal-weak, but did not assign a λ Boo type. Our spectral type A2 Ve kB9mB9 (λ Boo) is significantly different from that of Gray & Corbally (1998)—kB9 A0Va-(e)—suggesting a spectrum variable. See Pascual et al. (2016) for a plot of its SED.

HD 142994: A late-type λ Boo star showing significant excesses in the W2, W3, and W4 bands. The photometry in those bands is listed as "A" quality in the AllWISE Souce Catalog.

HD 154153: First classified as a λ Boo star by Paunzen (2001), this star has a late spectral type (F1) for a λ Boo star, but shows sizeable infrared excesses in the *WISE* W1 (3.35 μm) and W2 (4.6 μm) bands, and smaller excesses at W3 and W4. However, according to the AllWISE point-source catalog, that photometry *may* be contaminated by a halo from a nearby bright star. *Spitzer* IRAC 3.6 and 4.5 μm photometry, on the other hand, are consistent with no infrared excesses in that wavelength range.

HD 169142: Folsom et al. (2012) detected a "clear λ Boo pattern of abundances." Our spectrum shows clear infilling of the Hβ line as well as Hγ, as well as a clearly metal-weak character. The literature is unclear about the λ Bootis nature of this star (see Murphy et al. 2015), but our spectrum shows clear λ Boo characteristics. It appears to be a spectrum variable, and it would be of interest to follow this star for a period of time to see if its λ Bootis nature also varies. See Pascual et al. (2016) for a plot of its SED.

HD 183007: We concur with Murphy et al. (2015) that this star has a composite spectrum, but differ from them in not assigning a λ Boo type, largely because of the inconsistency between the K-line and the metallic-line types.

HD 188164: Classified by Paunzen et al. (1996) as λ Boo(?), but by Paunzen et al. (2001) as A3 V (e.g., normal), this star does appear from our spectra to be mildly metal-weak (A6 V kA2mA3). Murphy et al. (2015) consider it an extremely mild, but bona fide λ Boo star, although with the caveat that a full abundance analysis is necessary for certainty. We prefer to err on the cautious side, and call this star a possible, although very mild, λ Boo star. It is a spectroscopic binary and does show a slight excess in the *WISE* W2 band, although not at W3 or W4.

HD 217813: An A2 V shell star that shows IR excesses consistent with the presence of a cooler companion. Those IR excesses can be accounted for within the errors by a 4900K companion with a bolometric luminosity 0.6 times

that of the visible component. No parallax is available for HD 217813. Adopting $M_V = 1.9$ for the visible component (Gray & Corbally 2009) and applying appropriate bolometric corrections from Flower (1996), this yields, for the companion, $L = 8.7 L_\odot$, which would place the companion star at the base of the red-giant branch. The shell features in the spectrum may arise from mass transfer in this possible Algol system.

BD-13 6465: This star has been variously classified in the literature as a high-latitude spectroscopically peculiar star (A2pec, Graham & Slettebak 1973), a subdwarf sdB5 (deduced from Vilnius photometry, Bartkevicius & Lazauskaite 1997), and a young runaway star (Tetzlaff et al. 2011). Our spectral type, F1 V kA2mA3, suggests either a late-type λ Boo star or an F1 intermediate population II star. Its high galactic latitude ($-69°$) yields a very low reddening along its line of sight ($\sim$0.02 mag, Schlafly & Finkbeiner 2011). Assuming zero reddening, the *Gaia* parallax (3.01 $\pm$ 0.30 mas, *Gaia* Collaboration et al. 2016a, 2016b) implies an absolute magnitude $M_V = 2.97 \pm 0.21$. This, combined with $B - V = 0.29$, is consistent with an F-type dwarf. Its space velocity components relative to the local standard of rest are $U = -43\,\mathrm{km\,s^{-1}}$, $V = 2\,\mathrm{km\,s^{-1}}$, and $W = 0\,\mathrm{km\,s^{-1}}$, consistent with the young thin-disk population. An abundance analysis will be required to decide on the nature of this interesting star.

CD-31 306: This star has been classified in the literature as a blue straggler star (cf. Carney et al. 2005), a candidate HB star (Beers et al. 2007), and a carbon-enhanced metal-poor star (Preston & Sneden 2000). Our classification is F3 V kA2mA2 V, but the spectrum, which is clearly metal-weak, is sufficiently noisy that we cannot distinguish among those possibilities.

7. Discussion and Conclusions

A total of 45 "new" λ Boo stars (including a number of late-type λ Boo stars) have been classified in this paper. These 45 consist of 24 from the Tycho sample, 12 from Murphy et al.'s probable and uncertain categories, and 9 from the Strömgren $[m_1]$–$[c_1]$ technique. This represents a 70% increase in the number of known λ Boo stars, from the 64 identified in Murphy et al. (2015). Of course, the identification of these stars as members of the λ Boo class should be followed up with high-resolution abundance studies to confirm a λ Boo abundance pattern.

The Tycho sample, which is presumably unbiased with respect to infrared excesses, shows that, at least within the errors, λ Boo stars do not have a greater tendency than normal A-type stars to show infrared excesses out to 22 μm. However, this conclusion says nothing about the proportions that would be detected at longer wavelengths, and it will be an important follow-up to this paper to observe both the normal A-type stars and the λ Boo stars in the Tycho sample at longer wavelengths, once instruments with suitable sensitivities in the far-infrared become available again.

The existence of evolved (i.e., post-ZAMS) λ Bootis stars in both samples, some of which show evidence for debris disks, suggests that the λ Bootis "phenomenon" can operate either continuously or episodically over the main-sequence lifetime of an A-type star. Our hypothesis is that there are multiple mechanisms that could disturb a remnant Kuiper debris disk or Oort cloud, leading to collisions that would produce a renewed supply of volatiles and dust and subsequent accretion of metal-depleted gas. Such mechanisms could include the migration of massive planets and/or the close approach of a star. See also the discussion in Murphy & Paunzen (2017). With reference to the probability of an encounter with a star, Bailer-Jones (2015) has recently investigated close (within a fraction of a parsec) encounters of nearby stars with our own solar system. The implied time between sub-parsec encounters (a few Myr) is sufficiently close to the timescale for the persistence of the λ Boo abundance pattern after the cessation of accretion (see the Introduction) to make this an interesting possibility. It would be of interest to model this mechanism to understand if it can explain the frequency (2%) of λ Boo stars among the A-type stars.

The presence of significant infrared excesses for a number of late-type (F1 and later) λ Boo candidates reported in this paper suggests very strongly that λ Boo stars can exist at spectral types as late as F2 or F3. We, therefore, propose that the presence of infrared excesses in late-type λ Boo candidates is a potentially useful criterion for distinguishing these stars from metal-weak thick-disk stars.

We gratefully acknowledge support of National Science Foundation grants AST-1211213, AST-1211215, and AST-1211221. Q.S.R. gratefully acknowledges support from a North Carolina Space Grant Undergraduate Research Scholarship. We also acknowledge with gratitude time for four observing runs granted by the South African Astronomical Observatory. This research has made use of the NASA/IPAC Infrared Science Archive, which is operated by the Jet Propulsion Laboratory, California Institute of Technology, under contract with the National Aeronautics and Space Administration. Some of the data presented in this paper were obtained from the Mikulski Archive for Space Telescopes (MAST). STScI is operated by the Association of Universities for Research in Astronomy, Inc., under NASA contract NAS5-26555. Support for MAST for non-*HST* data is provided by the NASA Office of Space Science via grant NNX09AF08G and by other grants and contracts. This research has also made use of the SIMBAD database, operated at CDS, Strasbourg, France.

References

Abt, H. A. 1981, ApJS, 45, 437
Acke, B., & Waelkens, C. 2004, A&A, 427, 1009
Bailer-Jones, C. A. L. 2015, A&A, 575, A35
Bartkevicius, A., & Lazauskaite, R. 1997, BalA, 6, 499
Beers, T. C., Almeida, T., Rossi, S., Wilhelm, R., & Marsteller, B. 2007, ApJS, 168, 277
Bessell, M., & Murphy, S. 2012, PASP, 124, 140
Bowyer, S., Sasseen, T. P., Wu, X., & Lampton, M. 1995, ApJS, 96, 461
Bressan, A., Marigo, P., Girardi, L., et al. 2012, MNRAS, 427, 127
Carney, B. W., Latham, D. W., & Laird, J. B. 2005, AJ, 129, 466
Castelli, F., & Kurucz, R. L. 2003, in IAU Symp. 210, Modelling of Stellar Atmospheres, ed. N. E. Piskunov, W. W. Weiss, & D. F. Gray (San Francisco, CA: ASP), A20
Charbonneau, P. 1993, ApJ, 405, 720
Cheng, K.-P., Neff, J. E., Johnson, D. M., et al. 2017, AJ, 153, 39
Cowley, C. R., Hubrig, S., González, J. F., & Savanov, I. 2010, A&A, 523, A65
Draper, Z. H., Matthews, B. C., Kennedy, G. M., et al. 2016, MNRAS, 456, 459
Fitzpatrick, E. L. 1999, PASP, 111, 63
Flower, P. J. 1996, ApJ, 469, 355
Folsom, C. P., Bagnulo, S., Wade, G. A., et al. 2012, MNRAS, 422, 2072

Gaia Collaboration, Brown, A. G. A., Vallenari, A., et al. 2016a, A&A, 595, A2
Gaia Collaboration, Prusti, T., de Bruijne, J. H. J., et al. 2016b, A&A, 595, A1
Graham, J. A., & Slettebak, A. 1973, AJ, 78, 295
Gray, R. O. 1988, AJ, 95, 220
Gray, R. O. 1989, AJ, 98, 1049
Gray, R. O. 1991, in Precision Photometry, ed. A. G. Davis Philip, A. R. Upgren, & K. A. Janes (Philadelphia, PA: Davis), 309
Gray, R. O., & Corbally, C. J. 1993, AJ, 106, 632
Gray, R. O., & Corbally, C. J. 1994, AJ, 107, 742
Gray, R. O., & Corbally, C. J. 1998, AJ, 116, 2530
Gray, R. O., & Corbally, C. J. 2002, AJ, 124, 989
Gray, R. O., & Corbally, C. J. 2009, Stellar Spectral Classification (Princeton, NJ: Princeton Univ. Press)
Gray, R. O., & Corbally, C. J. 2014, AJ, 147, 80
Gray, R. O., Corbally, C. J., De Cat, P., et al. 2016, AJ, 151, 13
Gray, R. O., Corbally, C. J., Garrison, R. F., et al. 2006, AJ, 132, 161
Gray, R. O., Corbally, C. J., Garrison, R. F., McFadden, M. T., & Robinson, P. E. 2003, AJ, 126, 2048
Gray, R. O., & Kaye, A. B. 1999, AJ, 118, 2993
Griffin, R. E. M., Gray, R. O., & Corbally, C. J. 2012, A&A, 547, 8
Høg, E., Fabricius, C., Makarov, V. V., et al. 2000, A&A, 355, L27
Holweger, H., & Rentzsch-Holm, I. 1995, A&A, 303, 819
Holweger, H., & Stürenburg, S. 1991, A&A, 252, 255
Jura, M. 2015, AJ, 150, 166
Kama, M., Folsom, C. P., & Pinilla, P. 2015, A&A, 582, L10
Kurucz, R. L., & Bell, B. 1995, Kurucz CD-ROM 23, Atomic Line Data (Cambridge, MA: Smithsonian Astrophys. Obs.)
Lagrange-Henri, A. M., Vidal-Madjar, A., & Feriet, R. 1988, A&A, 190, 275
Marois, C., Macintosh, B., Barman, T., et al. 2008, Sci, 322, 1348
Martin, D. C., Fanson, J., Schiminovich, D., et al. 2005, ApJL, 619, L1
Matijevič, G., Zwitter, T., Munari, U., et al. 2010, AJ, 140, 184
Morgan, W. W., Keenan, P. C., & Kellman, E. 1943, An Atlas of Stellar Spectra (Chicago, IL: Univ. Chicago)
Murphy, S. J., Corbally, C. J., Gray, R. O., et al. 2015, PASA, 32, e036
Murphy, S. J., & Paunzen, E. 2017, MNRAS, 466, 546
Nichols, J. S., Henden, A. A., Huenemoerder, D. P., et al. 2010, ApJS, 188, 473
Nichols, J. S., & Linsky, J. L. 1996, AJ, 111, 517
Pascual, N., Montesinos, B., Meeus, G., et al. 2016, A&A, 586, A6
Paunzen, E. 2001, A&A, 373, 633
Paunzen, E., Duffee, B., Heiter, U., Kuschnig, R., & Weiss, W. W. 2001, A&A, 373, 625
Paunzen, E., & Gray, R. O. 1997, A&AS, 126, 407
Paunzen, E., Iliev, I. Kh., Fossati, L., Heiter, U., & Weiss, W. W. 2014, A&A, 567, A67
Paunzen, E., Iliev, I. Kh., Kamp, I., & Barzova, I. S. 2002, MNRAS, 336, 1030
Paunzen, E., Kamp, I., Weiss, W. W., & Wiesemeyer, H. 2003, A&A, 404, 579
Paunzen, E., Weiss, W. W., & Kuschnig, R. 1996, IBVS, 4302, 1
Pigulski, A., & Michalska, G. 2007, AcA, 57, 61
Preston, G. W., & Sneden, C. 2000, AJ, 120, 1014
Schlafly, E. F., & Finkbeiner, D. P. 2011, ApJ, 737, 103
Skrutskie, M. F., Cutri, R. M., Weinberg, M. D., et al. 2006, AJ, 131, 1163
Su, K. Y. L., Rieke, G. H., Stansberry, J. A., et al. 2006, ApJ, 653, 675
Tetzlaff, N., Neuhauser, R., & Hohle, M. M. 2011, MNRAS, 410, 190
Thureau, N. D., Greaves, J. S., Matthews, B. C., et al. 2014, MNRAS, 445, 2558
Turcotte, S., & Charbonneau, P. 1993, ApJ, 413, 376
Venn, K. A., & Lambert, D. L. 1990, ApJ, 363, 234
Waters, L. B. F. M, Trams, N. R., & Waelkens, C. 1992, A&A, 262, L37
Xue, M., Jiang, B. W., Gao, J., et al. 2016, ApJS, 224, 23